



HAL
open science

A multi-parametric recursive continuation method for nonlinear dynamical systems

Clément Grenat, Sébastien Baguet, Claude-Henri Lamarque, Régis Dufour

► **To cite this version:**

Clément Grenat, Sébastien Baguet, Claude-Henri Lamarque, Régis Dufour. A multi-parametric recursive continuation method for nonlinear dynamical systems. *Mechanical Systems and Signal Processing*, 2019, 127, pp.276-289. 10.1016/j.ymsp.2019.03.011 . hal-02067415

HAL Id: hal-02067415

<https://hal.science/hal-02067415>

Submitted on 14 Mar 2019

HAL is a multi-disciplinary open access archive for the deposit and dissemination of scientific research documents, whether they are published or not. The documents may come from teaching and research institutions in France or abroad, or from public or private research centers.

L'archive ouverte pluridisciplinaire **HAL**, est destinée au dépôt et à la diffusion de documents scientifiques de niveau recherche, publiés ou non, émanant des établissements d'enseignement et de recherche français ou étrangers, des laboratoires publics ou privés.

A multi-parametric recursive continuation method for nonlinear dynamical systems

C. Grenat^{a,b}, S. Baguet^{a,*}, C-H. Lamarque^b, R. Dufour^a

^aUniv Lyon, INSA-Lyon, CNRS UMR5259, LaMCoS, F-69621, France

^bUniv Lyon, ENTPE, CNRS UMR5513, LTDS, F-69518, France

Abstract

The aim of this paper is to provide an efficient multi-parametric recursive continuation method of specific solution points of a nonlinear dynamical system such as bifurcation points. The proposed method explores the topology of specific points found on the frequency response curves by tracking extremum points in the successive codimensions of the problem with respect to multiple system parameters. To do so, the characterization of extremum points by a constraint equation and its associated extended system are presented. As a result, a recursive algorithm is generated by successively appending new constraint equations to the extended system at each new level of continuation. Then, the methodology is applied to a nonlinear tuned vibration absorber (NLTVA). The limit of existence of isolated solutions and extremum points optimizing the region without isolated solution are found and used to improve the NLTVA.

Keywords: Harmonic balance method, Optimization, Continuation, Bifurcation tracking, Nonlinear vibration absorber, Isolated solutions.

1. Introduction

Continuation methods are efficient tools for parametric analysis and more specifically for tracking specific points such as bifurcations which govern the dynamical behavior of nonlinear systems. However, a mono-parametric analysis is sometimes not enough and multi-parametric continuation methods, i.e., when several or all parameters vary at the same time, are essential to properly analyze and design nonlinear systems. Nevertheless, a conventional multi-parametric continuation of solution points is almost unfeasible in practice because of the disproportionate computational time required to obtain the whole multi-dimensional solution surface. A more efficient approach consists in restricting this surface to a set of points or curves by means of additional constraint equations.

The method presented here consists in tracking branches of bifurcations with respect to several parameters by means of recursive continuation and augmented systems based on constraint equations characterizing extremum points. The key objective of the method is to explore the topology of specific points found on the frequency response curves by tracking extremum points in the successive codimensions of the problem. This provides useful information not only on the global dynamics of the system, but also on the way to tune the system parameters in order to improve it. The proposed algorithm combines multi-parametric continuation and bifurcation tracking. It is applied to a nonlinear tuned vibration absorber (NLTVA) with the aim of optimizing its safe operating region and making it more robust with respect to adverse dynamical phenomena such as isolated solutions (ISs). Some key references concerning each feature are given in the following literature review.

Various numerical methods can be found in the literature for the direct computation of periodic solutions. Amongst them, time domain approaches include the shooting method [1, 2, 3] and the orthogonal collocation technique [4] which consists in solving a nonlinear boundary value problem and are employed in softwares such as AUTO [5, 6], MATCONT [7], COLSYS [8], DDE-BIF [9] and COCO [10]. Concerning frequency domain approaches, the classical

*Corresponding author. Tel.: +33 4 72 43 81 93; fax: +33 4 78 89 09 80.

Email address: sebastien.baguet@insa-lyon.fr (S. Baguet)

method is the harmonic balance method (HBM) which expands the unknown state variables and nonlinear forces in truncated Fourier series. This method is very popular because of its efficiency and its versatility in handling nonlinearities. In the case of the HBM, the nonlinear terms are conveniently computed with the alternating frequency-time (AFT) method [11] which consists in going back and forth between time and frequency domains by means of Fourier transforms. Over time, many improvements have been introduced and the HBM can now handle systems with many types of nonlinearity such as the non-differential [12] and the non-smooth ones [13, 14]. The efficiency of the method has been enhanced by adaptive schemes such as the automatic selection of harmonics of interest [15, 16]. The method also has been extended to quasi-periodic solutions [17, 18, 19, 20].

Coupled with a continuation technique, these methods provide the equilibrium curve of periodic solutions with respect to a varying system parameter. Two main continuation techniques are used, the pseudo arc-length continuation based on tangent prediction steps and on orthogonal corrections [21, 22, 3] and the asymptotic numerical method [23].

At some specific points, the stability of the periodic solution is ill-posed and the implicit function theorem is invalidated. Such points, called bifurcations, are indicative of multiple solutions, amplitude jumps, loss of stability, change of dynamical regime, quasi-periodicity, chaos, etc. [3]. Their precise computation is therefore of high interest. Bifurcation points are computed with two main classes of algorithms. The first one comprises the so-called minimally extended systems which add to the equilibrium equation a single scalar equation defined with a bordering technique. The other class relies on standard extended systems which add a set of equations characterizing the bifurcation by means of the eigenvectors. Codimension 1 bifurcations found on limit cycles are composed of Limit Points (LPs), Branch Points (BPs) and Neimark-Sacker points (NSs). LP bifurcations are associated with dynamical phenomena such as loss of stability, amplitude jumps or generation of ISs that can lead to unexpected behavior. The first calculation of LPs with standard extended systems was proposed by Seydel [24, 25], then by Moore and Spence [26] and Wriggers and Simo [27] amongst others. The calculation of LPs with minimally extended systems was first proposed by Griewank and Reddien [28], then used in multiple works [29, 30]. The coupling of standard extended systems with HBM was developed by Petrov [31] in the case of branch points and by Xie *et al.* [32] in the case of LPs.

Bifurcation tracking provides an efficient parametric analysis and permits a better understanding of the complexity of the dynamical behavior of nonlinear systems. LP tracking was first carried out by Jepson and Spence [33] with standard extended systems. It was also used to analyze the sensitivity of critical buckling loads to imperfections [34, 35, 36]. The codimension-1 bifurcation tracking for dynamical systems has been incorporated in several softwares. Algorithms based on minimally extended systems can be found in the books of Kuznetsov [37] and Govaerts [38] and have been implemented in the MATCONT software [7]. On the other hand, the bifurcation tracking based on standard extended systems is used in softwares such as AUTO [6], LOCA [39], COCO [10]. The tracking of codimension-1 bifurcations points using minimally extended system combined with the HBM with application to large-scale mechanical systems was proposed by Detroux *et al.* [40]. Xie *et al.* [41] implemented the continuation of LPs and Neimark-Sacker bifurcations using standard extended systems and HBM to analyze a nonlinear energy sink (NES) and a nonlinear Jeffcott rotor.

When dealing with nonlinear systems, one-parameter continuation methods may be too limited because system parameters are often inter-correlated. Therefore, multi-parametric continuation methods are interesting tools for analyzing the behavior of a system when several or all the parameters vary. To develop such a method, additional constraint equations need to be appended to the extended system in order to free additional system parameters. Constraint equations characterizing extremum points are good candidates for this purpose. In this case, multi-parametric continuation methods are close to the methods of the literature dealing with optimization. Several references deal with optimization algorithms coupled with continuation techniques to provide new multi-parametric methods. For instance, it was used in homotopy techniques where a small parameter is introduced to link two problems. This technique was notably used in optimization for smoothing techniques [42, 43, 44] and for the fitting of optimal system kinematics [45, 46]. Continuation methods were also used to explore the topology of extremums for large parametric deformations [47]. The methods resulting from the coupling of optimization algorithm and continuation techniques have since been extended in several directions such as multi-parametric algorithms, recursive methods and critical set point analysis [48, 49]. Concerning multi-parametric algorithms, Wolf and Sanders [50] proposed a multi-parametric homotopy technique for computing operating points of nonlinear circuits. Then, Vanderbeck [51] used a multi-parametric optimization by recursion to optimize a manufacturing cutting process. Recursivity-based optimization was addressed by Schütze *et al.* [52] who proposed a recursive subdivision technique to perform multi-objective and multi-parametric optimization. Since then, multi-parametric optimization was coupled with continuation, Kernevez *et al.* [53] used a

descent optimization algorithm coupled with a continuation method to perform the optimization of nonlinear systems. Later, Balaram *et al.* [54] combined the method of Kernevez *et al.* with a genetic algorithm in order to provide a global algorithm of optimization by continuation. They used this method to minimize the acceleration of a Duffing oscillator and to tune nonlinear vibration absorbers.

In the literature, the NLTVA was used for many applications. Wang [55] tuned a NLTVA to minimize the critical limiting depth induced by chatter during machining process. An optimized hysteretic NLTVA was used by Carpineto *et al.* [56] for minimizing the vibrations of structures. Detroux *et al.* [57] optimized a NLTVA by generalizing Den Hartog's equal-peak method to nonlinear systems. The NLTVA was also used for the passive control of an airfoil flutter instability by Mahler *et al.* [58] who optimized a NLTVA to push the appearance of the post-critical regime at higher flux velocities.

Besides its advantageous properties, the NLTVA also presents some unwanted adverse dynamical phenomena such as the generation of ISs. These isolated resonance curves are periodic solutions detached from the main response curves. They are therefore difficult to compute by simply continuing the main response curves. In order to properly design nonlinear systems, it is important to be able to detect these ISs which were first studied in 1951 by Abramson [59]. Since then, several scenarios for the creation of ISs have been revealed. DiBerardino and Dankowicz [60] showed that ISs can be created by introducing asymmetry into a nonlinear system. In [61], the presence of IS is explained analytically by analyzing the 1:3 internal resonance configuration between two Duffing oscillators for different couplings. In [62], an experiment was carried out to illustrate the IS phenomenon between a Duffing oscillator and a clamped-clamped beam at a 1:3 internal resonance configuration. In both papers, the frequency gap between the response curve and the IS was calculated and explained by means of phase-locking. Gatti investigated a mechanical system composed of a primary mass linked with a nonlinear coupling to a smaller second mass. He used analytical methods to compute frequency response curves of coupled oscillators and uncovered IS [63] and then used LP curves to predict the appearance of IS [64]. These researches have since been applied to a nonlinear vibration absorber to predict its dynamics while reducing the vibration of the primary mass [65, 66]. Detroux *et al.* [67] presented a method to localize the ISs in a NLTVA using LP continuation. The presence of ISs was also explained with NNM continuation and internal resonances. In [68], Hill *et al.* calculated the NNMs of a NLTVA system composed of a Duffing oscillator coupled to a linear oscillator with a cubic restoring force. They used an energy balance method to link the energy of the modes to the amplitude of the force to be injected into the damped system in order to obtain a frequency response curve with the same level of energy. By superimposing the obtained NNM with the response curve, IS phenomenon was explained by means of internal resonances. By using singularity theory and HBM, Habib *et al.* [69] analyzed the mechanism of IS creation in a Duffing oscillator with nonlinear damping and demonstrated the link between the damping force and ISs. The same singularity theory was used by Cirillo *et al.* [70] to study IS topology based on hysteresis, bifurcation and isola center points.

Some references dealing with IS optimization also exist. For a NES system, Starosvetsky and Gendelman [71] showed that it is possible to remove ISs by adding a well tuned piece-wise quadratic damping into the mechanical system. Gourc *et al.* [72] showed that ISs can be removed while conserving the energy pumping property by working on the values of the system parameters. Concerning the NLTVA, Cirillo *et al.* [70] showed that a fifth order nonlinear spring can be tuned to remove the ISs generated by the cubic nonlinearity. However, it turned out that ISs can be generated when increasing the order of the nonlinear additional spring. Kernevez *et al.* [53] proposed a continuation-based algorithm to control the position of ISs in a reaction-diffusion chemical system. Their strategy consisted in following curves of isola centers with respect to one system parameter.

The method presented here is intended as an extension of [41] to the multi-parametric case. The method of Kernevez *et al.* [53] can be viewed as a particular case of this method and corresponds to the second level of recursivity of limit points. Unlike the method in [53], the proposed algorithm is not restricted to limit points and can deal with any of the bifurcations presented in [41]. Also, a practical tool being able to track in a recursive way the branches of bifurcations with respect to several parameters inside a unique execution of a code (one computation) is completely new.

This paper is organized as follows. In Section 2, the notion of extremum point is used to propose an original multi-parametric recursive continuation method. First, the characterization of extremum points by a constraint equation and its associated extended system are presented. Then, a recursive algorithm is generated by successively appending new constraints equations to the extended system at each new level of continuation, i.e., when a new parameter is freed. In Section 3, the multi-parametric recursive continuation method is used to calculate the limit of existence of ISs in the

case of a NLTVA and to improve its efficiency by optimizing the safe operating range. Finally, conclusions are drawn in Section 4.

2. Multi-parametric recursive continuation

2.1. Extremum point

Let the following problem be considered:

$$\mathbf{G}(\mathbf{Y}, \alpha) = \mathbf{0} \quad (1)$$

defining a curve depending on the state variables $\mathbf{Y} \in \mathbb{R}^n$ and parametrized by a set of system parameters $\alpha \in \mathbb{R}^p$. Let assume that locally the curve has a local extremum with respect to one system parameter $\alpha_1 \in \alpha$ characterized by:

$$\Delta\alpha_1 = 0 \quad (2)$$

with $\Delta\alpha_1$ the variation of α_1 . The first variation of the problem (1) gives:

$$\frac{\partial \mathbf{G}}{\partial \mathbf{Y}} \Delta \mathbf{Y} + \frac{\partial \mathbf{G}}{\partial \alpha_1} \Delta \alpha_1 = \mathbf{0} \quad (3)$$

with $\Delta \mathbf{Y}$ the variation of \mathbf{Y} . Combined with Eq. (2), the following relationship is obtained:

$$\frac{\partial \mathbf{G}}{\partial \mathbf{Y}} \Delta \mathbf{Y} = \mathbf{0} \quad (4)$$

From Eq. (3), the following scalar equation is obtained:

$$\Delta \mathbf{Y}^T \frac{\partial \mathbf{G}}{\partial \mathbf{Y}} \Delta \mathbf{Y} + \Delta \mathbf{Y}^T \frac{\partial \mathbf{G}}{\partial \alpha_1} \Delta \alpha_1 = 0 \quad (5)$$

According to the implicit function theorem, the variation $\Delta\alpha_1$ is defined if and only if $\Delta \mathbf{Y}^T \frac{\partial \mathbf{G}}{\partial \alpha_1}$ is not null. Therefore, the problem composed of Eqs. (1) and (2) is equivalent to the following extended system:

$$\begin{cases} \mathbf{G}(\mathbf{Y}, \alpha) = \mathbf{0} \\ \frac{\partial \mathbf{G}}{\partial \mathbf{Y}} \boldsymbol{\phi} = \mathbf{0} \\ \boldsymbol{\phi}^T \frac{\partial \mathbf{G}}{\partial \alpha_1} \neq 0 \end{cases} \quad (6)$$

with $\boldsymbol{\phi} \in \mathbb{R}^n$.

The condition $\boldsymbol{\phi}^T \frac{\partial \mathbf{G}}{\partial \alpha_1} \neq 0$ that insures $\Delta\alpha_1 = 0$ can be seen as a non-degeneracy condition avoiding degenerated points which result in an ill-conditioned jacobian during continuation. However, some of these degenerated points are calculated during the recursive continuation in increasing codimension. Therefore, the augmented system (6) characterizing the extremum points when $\boldsymbol{\phi}^T \frac{\partial \mathbf{G}}{\partial \alpha_1} \rightarrow 0$ must be extended in order to also support such degenerated points.

When $\boldsymbol{\phi}^T \frac{\partial \mathbf{G}}{\partial \alpha_1} \rightarrow 0$, a normalization equation has to be added to the augmented system (6) in order to avoid the trivial solution $\boldsymbol{\phi} = \mathbf{0}$ and thus an ill-posed problem, leading to the following extended augmented system:

$$\begin{cases} \mathbf{G}(\mathbf{Y}, \alpha) = \mathbf{0} \\ \frac{\partial \mathbf{G}}{\partial \mathbf{Y}} \boldsymbol{\phi} = \mathbf{0} \\ \boldsymbol{\phi}^T \frac{\partial \mathbf{G}}{\partial \alpha_1} = 0 \\ \boldsymbol{\phi}^T \boldsymbol{\phi} - 1 = 0 \end{cases} \quad (7)$$

In order to obtain an augmented system that provides both degenerated and non generated extremum points, the equation associated with the degeneracy characterization has to be withdrawn.

$$\begin{cases} \mathbf{G}(\mathbf{Y}, \alpha) = \mathbf{0} \\ \frac{\partial \mathbf{G}}{\partial \mathbf{Y}} \boldsymbol{\phi} = \mathbf{0} \\ \boldsymbol{\phi}^T \boldsymbol{\phi} - 1 = 0 \end{cases} \quad (8)$$

With an augmented system supporting the degeneracy, the robustness of the continuation of extremum points is improved. Moreover, this system has the same structure as the standard extended system used to characterize LP bifurcations [32].

2.2. Recursive continuation of extremum points in increasing codimension.

The multi-parametric recursive continuation method is based on the recursivity of the extended system (8).

Initialization of the recursive continuation. The recursive continuation is started from a solution point \mathbf{Y}_0 characterized by an extended system $\mathbf{G}_0(\mathbf{Y}_0) = \mathbf{0}$, e.g., a bifurcation point or an extremum point (see [41] for the definition of such an extended system). For instance, if a LP of an equilibrium branch is chosen as starting point, the extended system can be written as:

$$\mathbf{G}_0(\mathbf{Y}_0) = \begin{pmatrix} \mathbf{R}(\mathbf{X}, \omega) \\ \frac{\partial \mathbf{R}}{\partial \mathbf{X}} \boldsymbol{\phi}_0 \\ \boldsymbol{\phi}_0^T \boldsymbol{\phi}_0 - 1 \end{pmatrix} = \mathbf{0}_{2L+1} \quad (9)$$

where the subsystem $\mathbf{R}(\mathbf{X}, \omega) = \mathbf{0}_L$ is the equilibrium equation, and $\mathbf{Y}_0 = (\mathbf{X}, \boldsymbol{\phi}_0, \omega)$ with \mathbf{X} the vector of L unknown variables, $\boldsymbol{\phi}_0$ the null right eigenvector of the jacobian $\frac{\partial \mathbf{R}}{\partial \mathbf{X}}$ and ω a system parameter.

Recursive continuation. A system parameter $\alpha_1 \in \alpha$ is then considered as a new unknown and the branch of solutions of the system $\mathbf{G}_0(\mathbf{Y}_0, \alpha_1) = \mathbf{0}_{2L+1}$ is followed with a continuation method. During the continuation, an extremum point is detected when $\Delta \alpha_1 = 0$. The extremum point at the first level of continuation is called 1-extremum point. To locate this point more precisely, an extended system similar to Eq. (8) is used:

$$\mathbf{G}_1(\mathbf{Y}_1) = \begin{pmatrix} \mathbf{G}_0(\mathbf{Y}_0, \alpha_1) \\ \frac{\partial \mathbf{G}_0}{\partial \mathbf{Y}_0} \boldsymbol{\phi}_1 \\ \boldsymbol{\phi}_1^T \boldsymbol{\phi}_1 - 1 \end{pmatrix} = \mathbf{0}_{4L+3} \quad \text{with} \quad \mathbf{Y}_1 = (\mathbf{Y}_0, \boldsymbol{\phi}_1, \alpha_1) \quad (10)$$

Then, another parameter $\alpha_2 \in \{\alpha \setminus \alpha_1\}$ is considered as a new unknown and the branch of solutions of $\mathbf{G}_1(\mathbf{Y}_1, \alpha_2) = \mathbf{0}_{4L+3}$ is followed in order to find its extremum points with respect to parameters \mathbf{Y} , α_1 and α_2 . This procedure is repeated in a recursive manner until all the parameters in the set α have been used. In the following, the extremum points found at the k^{th} level of continuation are called k -extremum points. During the continuation of $\mathbf{G}_{k-1}(\mathbf{Y}_{k-1}, \alpha_k)$, the k -extremum points with respect to α_j , $j = 1 \dots k$ are detected with $\Delta \alpha_j = 0$ and then precisely located by solving:

$$\mathbf{G}_k(\mathbf{Y}_k) = \begin{pmatrix} \mathbf{G}_{k-1}(\mathbf{Y}_{k-1}, \alpha_k) \\ \frac{\partial \mathbf{G}_{k-1}}{\partial \mathbf{Y}_{k-1}} \boldsymbol{\phi}_k \\ \boldsymbol{\phi}_k^T \boldsymbol{\phi}_k - 1 \end{pmatrix} = \mathbf{0}_{2^{k+1}(L+1)-1} \quad \text{with} \quad \begin{array}{l} \mathbf{Y}_k = (\mathbf{Y}_{k-1}, \boldsymbol{\phi}_k, \alpha_k) \\ \mathbf{Y}_{k-1}^j = ((\mathbf{Y}_{k-1}, \alpha_k) \setminus \alpha_j, \alpha_k) \end{array} \quad (11)$$

In summary, the extended system (8) characterizing extremum points is used to create a recursive extended system characterizing extremum points in increasing dimension. By using such a recursive characterization of extremum points, a multi-parametric recursive continuation method can be implemented and applied to any specific point characterized by the initial augmented system $\mathbf{G}_0(\mathbf{Y}_0)$.

2.3. Algorithm and results interpretation

In order to recursively obtain all the branches of extremum points by continuation with respect to a predefined set of parameters, the algorithm presented in Tab. 1 is used.

The branches of extremum points obtained with the recursive continuation form a tree with ramifications indicating increasing codimensions. The tree of extremum points can be used to find local optimal sets of system parameters α , while the surrounding branches form a topological skeleton defining the global dynamics of the system. In more concrete terms, this skeleton can be used for instance to find the values of the parameters α for which specific bifurcation points appear or collapse, i.e. by extension, the range of values for which such points exist. This knowledge can then be exploited to appropriately choose the value of the system parameters and insure a safe design.

Step 0:	<p>Initialization</p> <ul style="list-style-type: none"> - Choose the set of system p parameters $\alpha = (\alpha_1, \dots, \alpha_p)$ to use for the multi-parametric recursive continuation. - Define the bounded domain $D_\alpha = D_{\alpha_1} \times \dots \times D_{\alpha_p}$ in which the set of parameters α is allowed to vary. - Solve the extended system $G_0(Y_0) = \mathbf{0}_{2L+1}$ to locate the selected initial point Y_0 to be continued recursively.
Step 1:	<p>Level 1 of continuation and detection of 1-extremums</p> <p>(a) Level 1 of continuation</p> <ul style="list-style-type: none"> * Consider α_1 as a new unknown. * Continue the branch $G_0(Y_0, \alpha_1) = \mathbf{0}$ with α_1 spanning D_{α_1} * Detect all the 1-extremum points with the indicator $\Delta_{\alpha_1} = 0$ <p>(b) Solve the extended system $G_1(Y_1) = \mathbf{0}$ to precisely locate all the 1-extremums Y_1.</p> <p>(c) End the algorithm if no 1-extremum is detected. Otherwise, go to step 2.</p>
Step k : $k = [2, \dots, p]$	<p>Level k of continuation and detection of k-extremums</p> <p>For each $(k - 1)$-extremum Y_{k-1} located during step $k - 1$:</p> <p>(a) Level k of continuation</p> <ul style="list-style-type: none"> * Consider α_k as a new unknown. * Continue the branch $G_{k-1}(Y_{k-1}, \alpha_k) = \mathbf{0}$ with α_k spanning D_{α_k} * Detect all the k-extremums with respect to each parameter $\alpha_j \in [\alpha_1, \dots, \alpha_k]$ with the indicators $\Delta\alpha_j = 0$ <p>(b) Solve the extended system $G_k(Y_k) = \mathbf{0}$ to precisely locate all the k-extremum points Y_k detected in (a)</p> <p>(c) End the algorithm if no k-extremum is detected or if $k = p$. Otherwise, go to step $(k + 1)$.</p>

Table 1: Algorithm of the multi-parametric recursive continuation method

3. Multi-parametric analysis of ISs in a NLTVA

In this section, a two degrees-of-freedom NLTVA is considered. Despite its small number of degrees of freedom, it exhibits a complex behaviour including limit points, Neimark-Sacker bifurcations and isolated solutions. This system was already investigated in several papers (see [57] for instance) and a mono-parametric bifurcation analysis was proposed in [67]. Here, a multi-parametric bifurcation analysis is performed, from which the limits of existence of ISs are obtained. The HBM is applied to the mechanical model and standard extended systems are used to characterize LP bifurcations. Then, the recursive continuation method presented in Section 2 is applied to these LPs. The recursive continuation is composed of three levels of continuation with respect to a subset of three system parameters: the amplitude f_0 of the applied force, the nonlinear stiffness coefficient knl_2 and the damping coefficient c_2 of the NLTVA. On the first level, the LPs are continued with respect to the amplitude of the force f_0 . This level is used to explain the birth and merging of ISs. On the second level, the birth and merging points of the ISs are tracked with respect to the previous subset of parameters plus the nonlinear stiffness coefficient knl_2 of the vibration absorber as additional parameter. Finally, on the third level, the extremum points, where birth and merging of the ISs occur simultaneously, are followed with respect to the previous subset of parameters plus the damping coefficient c_2 of the absorber. Finally, it is shown how the results of the multi-parametric tracking can be used to optimize the dynamical behavior of the NLTVA and for robust design by identifying sets of parameters insuring safe operating conditions.

3.1. NLTVA Model

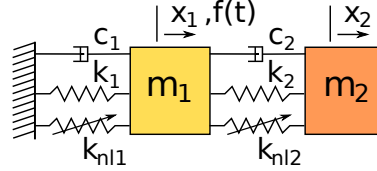


Figure 1: NLTVA mechanical model

A Duffing oscillator coupled with an attached NLTVA, as depicted in Fig. 1, is studied. The NLTVA system is a Duffing oscillator tuned in such a way as to absorb the energy vibration from the forced primary mass m_1 . The nonlinear dynamical behavior of the system is governed the following set of equations:

$$\begin{aligned} m_1 \ddot{x}_1 + c_1 \dot{x}_1 + k_1 x_1 + k_{nl1} x_1^3 + c_2 (\dot{x}_1 - \dot{x}_2) + k_2 (x_1 - x_2) + k_{nl2} (x_1 - x_2)^3 &= f_0 \cos \omega t \\ m_1 \epsilon \ddot{x}_2 + c_2 (\dot{x}_2 - \dot{x}_1) + k_2 (x_2 - x_1) + k_{nl2} (x_2 - x_1)^3 &= 0 \end{aligned} \quad (12)$$

with k_1 and k_2 the stiffness coefficients of the linear springs, k_{nl1} and k_{nl2} the coefficients of the nonlinear elastic forces, c_1 and c_2 the damping coefficients, $\epsilon = m_2/m_1$ the mass ratio. The primary mass is periodically forced at frequency ω and amplitude f_0 . The parameters of the primary system are set as follows: $\epsilon = 0.05$, $m_1 = 1\text{kg}$, $c_1 = 0.002\text{Ns/m}$, $k_1 = 1\text{N/m}$, $knl_1 = 1\text{N/m}^3$ in accordance with the literature [57]. The NLTVA parameters k_2 , c_2 , knl_2 are set according to the nonlinear generalization of the Equal-Peak method presented in [57]:

$$\begin{aligned} k_2^{opt} &= \frac{8\epsilon k_1 [16 + 23\epsilon + 9\epsilon^2 + 2(2+\epsilon)\sqrt{4+3\epsilon}]}{3(1+\epsilon)^2(64+80\epsilon+27\epsilon^2)} \approx 0.0454 \quad [N/(m.kg)] \\ k_{nl2}^{opt} &= \frac{2\epsilon^2 k_{nl1}}{1+4\epsilon} \approx 0.0042 \quad [N/(m^3.kg)] \\ c_2^{opt} &= \sqrt{\frac{k_2 m_2 (8+9\epsilon-4\sqrt{4+3\epsilon})}{4(1+\epsilon)}} \approx 0.0128 \quad [Ns/(m.kg)] \end{aligned} \quad (13)$$

The nonlinear equations of the NLTVA are then written in the following matrix form:

$$\mathbf{r}(\mathbf{x}, \omega, t) = \mathbf{M}\ddot{\mathbf{x}}(t) + \mathbf{C}\dot{\mathbf{x}}(t) + \mathbf{K}\mathbf{x}(t) + \mathbf{f}_{nl}(\mathbf{x}) - \mathbf{f}(\omega, t) = \mathbf{0} \quad (14)$$

The vector $\mathbf{x}(t)$ gathers the displacements of the $n = 2$ DOFs, $\boldsymbol{\alpha}$ is the vector of the system parameters. The matrices \mathbf{M} , \mathbf{C} , \mathbf{K} correspond to the mass, damping and stiffness matrix, \mathbf{f}_{nl} represents the non linear forces and \mathbf{p} the periodic

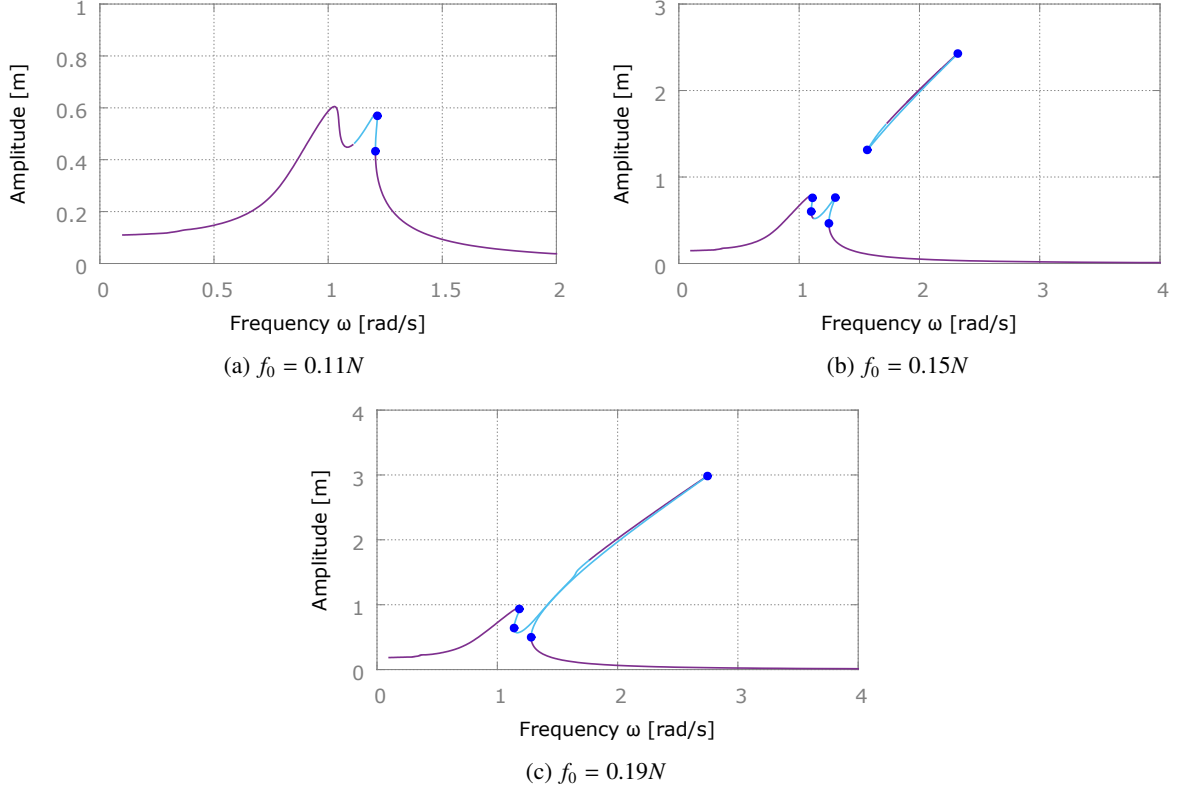


Figure 2: Frequency response curves of x_1 for $f_0 = [0.11, 0.15, 0.19]N$. Stable (Purple), Unstable (light blue), LP (dark blue ●)

excitation at frequency ω . By applying the HBM to the differential Eq. (14) as detailed in [32], the following nonlinear algebraic system of size $L = n(2H + 1)$ in the frequency domain is obtained:

$$\mathbf{R}(\mathbf{X}, \omega) = \mathbf{Z}(\omega)\mathbf{X} + \mathbf{F}_{nl}(\mathbf{X}) - \mathbf{F} = \mathbf{0} \quad (15)$$

with

$$\mathbf{Z}(\omega) = \omega^2 \nabla^2 \otimes \mathbf{M} + \omega \nabla \otimes \mathbf{C} + \mathbf{I}_{2H+1} \otimes \mathbf{K} = \text{diag}(\mathbf{K}, \mathbf{Z}_1, \dots, \mathbf{Z}_j, \dots, \mathbf{Z}_H) \quad (16)$$

$$\mathbf{Z}_j = \begin{bmatrix} \mathbf{K} - j^2 \omega^2 \mathbf{M} & \omega \mathbf{C} \\ -\omega \mathbf{C} & \mathbf{K} - j^2 \omega^2 \mathbf{M} \end{bmatrix}$$

where \otimes stands for the Kronecker tensor product. The nonlinear frequency response curves of the system for a fixed initial set of parameters (ω, α) and various amplitudes of forcing are then obtained by coupling Eq. (15) with a continuation procedure such as a pseudo arc-length technique [21, 41]. During the continuation, the evaluation in the frequency domain of the nonlinear forces \mathbf{F}_{nl} and their Jacobian matrices required for the Newton-Raphson iterations is performed with the so-called alternating frequency time (AFT) method [11].

3.2. Level-1 of LP continuation: ISs of the NLTVA

The parametric analysis is performed on the system (12), which possesses ISs for some ranges of parameters. The objective here is to characterize and track ISs in order to identify three regions: without IS, with unmerged IS and with merged IS. In order to show the ISs and their various behaviors, the frequency response curves of the NLTVA are plotted in Fig. 2 for $f_0 = [0.11, 0.15, 0.19]N$. For the lowest value of f_0 , there is no IS. Then, an IS appears for a slightly higher f_0 and finally merges for higher values of f_0 . Detroux *et al.* [67] have shown that it is possible to

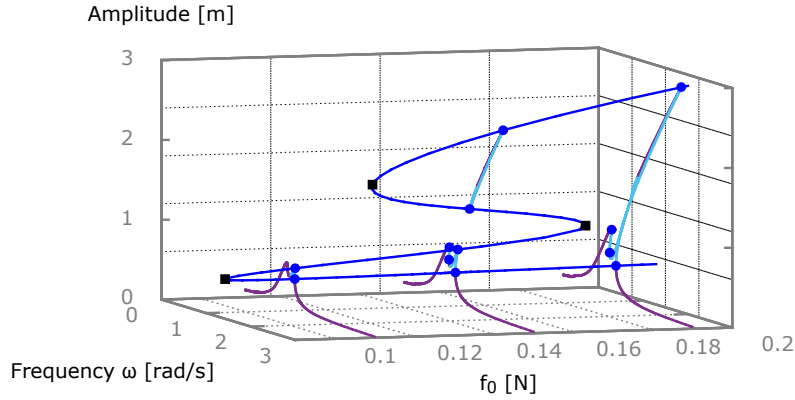


Figure 3: Continuation of LPs (Level 1). Stable (Purple), Unstable (light blue), LP (dark blue ●), 1-extremum (black ■)

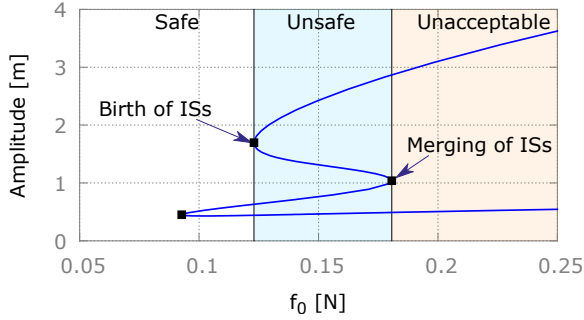


Figure 4: Continuation of LPs in the amplitude- f_0 plane. LP (dark blue solid line), 1-extremum (Black ■)

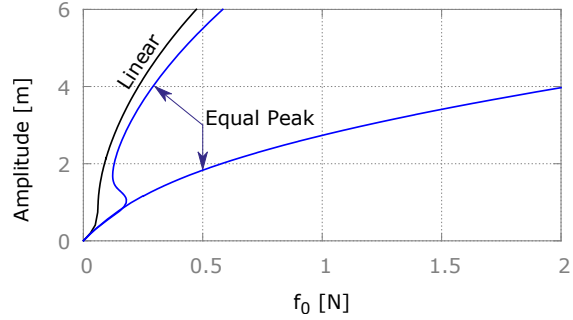


Figure 5: Continuation of the maximum of amplitude. Linear $k_{nl2} = 0$ (black), Equal peak $k_{nl} = 0.0042N/m^3$

characterize the birth and merging of ISs by tracking LP bifurcations with respect to f_0 using the extended system $\mathbf{G}_0(\mathbf{Y}_0, f_0) = \mathbf{0}$ described in Subsection 2.2.

To perform the parametric analysis of the ISs, the multi-parametric recursive continuation method is applied to the NLTVA model with a LP detected on a frequency response curve as initial point for the method. The continuation is performed with respect to the following set of system parameters: the forcing amplitude f_0 , the coefficients of nonlinear stiffness k_{nl2} and damping c_2 . This results in three levels of recursive continuation depending on the number of parameters varying during the continuation. At level 1, LPs are continued with respect to f_0 . At level 2, the birth and merging points of ISs are continued with respect to (f_0, k_{nl2}) . At level 3, the points where ISs appear and merge simultaneously are continued with respect to (f_0, k_{nl2}, c_2) .

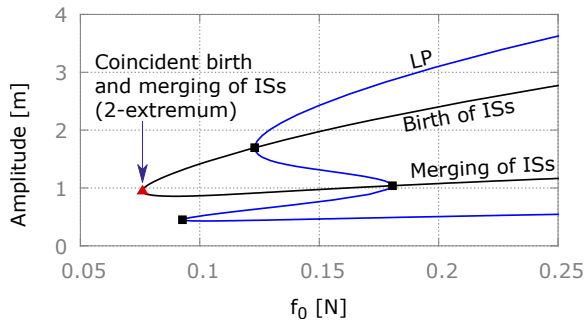
The branch of LPs obtained at level 1 is plotted in Fig. 3, while Fig. 4 shows its projection onto the amplitude- f_0 plane. One can see that the two extremum points obtained when $\Delta f_0 = 0$ characterize the birth ($f_0 = 0.12N$) and the merging ($f_0 = 0.18N$) of ISs. Following the classification introduced by Detroux *et al.* [67], three regions with different dynamical behaviors are characterized as follows: "Safe" when the response curve has no IS, "Unsafe" when the response curve exhibits an IS and "Unacceptable" when the IS has merged with the response curve. Concerning the "Safe" region, there is no IS for any value of the applied force f_0 , i.e., there is no possibility of jumping onto a higher amplitude stable solution. Conversely, inside the "Unsafe" region, ISs with higher amplitude exist. Therefore, this region presents a risk of jumping onto a stable solution at high amplitude. Finally the last region is called "Unacceptable" because the IS has already merged with the response curve and exhibits high amplitude solutions. There is no IS in the "Safe" and "Unacceptable" region since ISs regions either do not exist or have already merged. Fig. 5 shows that the amplitude of the primarily mass is much more attenuated with the equal peak design compared

to a design of the vibration absorber without any nonlinearity ($knl_2 = 0$). Moreover, the vibration absorber under equal peak design remains more efficient even after the merging of the ISs.

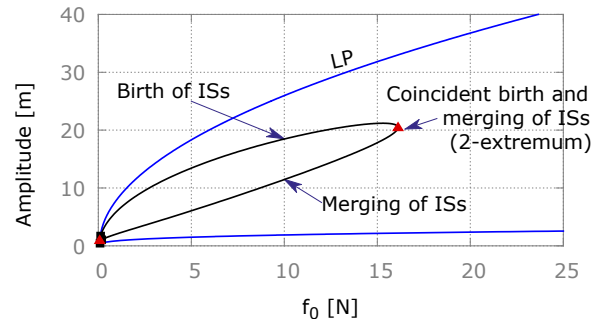
3.3. Level-2 of LP continuation: continuation of the coincident birth and merging of ISs

Once the 1-extremum points characterizing the birth and merging of ISs have been precisely located with the extended system (10), they can be followed by considering the nonlinear stiffness coefficient knl_2 as a new variable and computing the branch of solutions of $\mathbf{G}_1(\mathbf{Y}_1, knl_2) = \mathbf{0}$. The subset of varying parameters at level 2 is then (f_0, knl_2) . The resulting branch of 1-extremum points is plotted in Figs. 6 and 7.

Figs 6a and 6b show the branch for the same range of parameters as before whereas Figs 7a and 7b show an extended view of the whole branch of 1-extremum points. Two 2-extremum points can be observed on these extended views. The point at high amplitude of forcing represents the upper limit of existence of ISs, whereas the point at low amplitude of forcing represent the lower limit of existence of ISs. At these points, the birth and merging of ISs are coincident, i.e., the unsafe region has disappeared. For values of f_0 between these two points, ISs exist and for values of f_0 below and above, there is no IS. The level-2 extended system (11) $\mathbf{G}_2(\mathbf{Y}_2) = \mathbf{0}$ is used to locate precisely these two points leading to sets of parameters (f_0, knl_2) approximately equal to $(0.0076N, 0.0017N/m^3)$ and $(16N, 0.0076N/m^3)$. To better visualize the absence of the unsafe region at these two 2-extremums, the branches of LP for these sets of parameters are plotted in Figs. 8a and 8b.

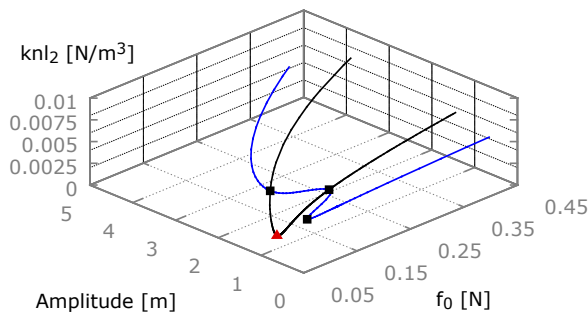


(a) Continuation of the birth and merging of ISs in the amplitude- f_0 plane

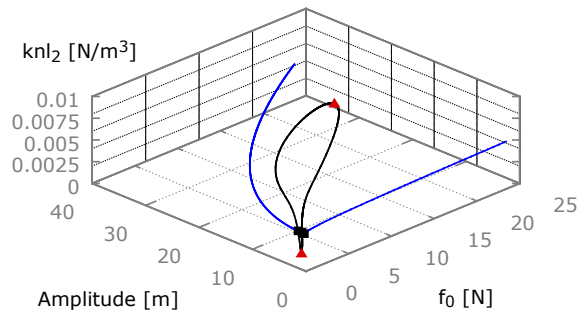


(b) Continuation of the birth and merging of ISs in the amplitude- f_0 plane (Extended view)

Figure 6: 2D-Continuation of birth and merging points (1-extremum, black solid line). LP (dark blue solid line), 1-extremum (black ■), 2-extremum (red ▲)

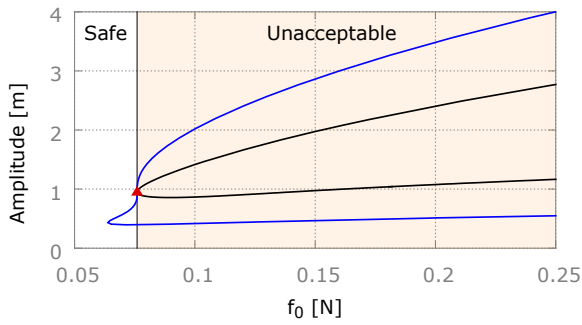


(a) 3D-Continuation of the birth and merging of ISs

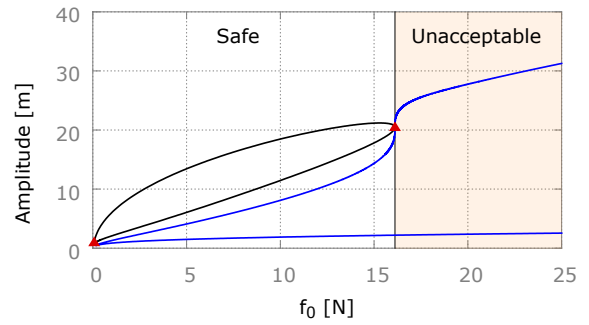


(b) 3D-Continuation of the birth and merging of ISs (Extended view)

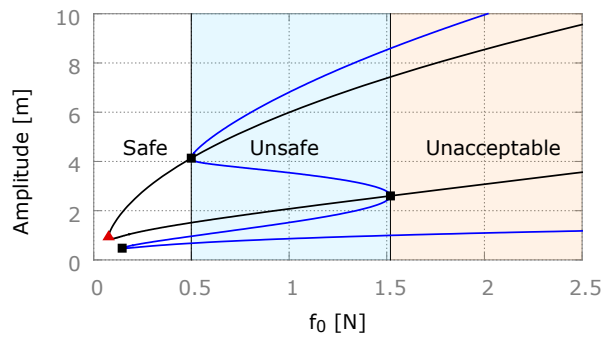
Figure 7: 3D-Continuation of birth and merging points (1-extremum, black solid line). LP (dark blue solid line), 1-extremum (black ■), 2-extremum (red ▲)



(a) LP curve for $knl_2 \approx 0.0017N/m^3$



(b) LP curve for $knl_2 \approx 0.0076N/m^3$



(c) LP curves for $knl_2 \approx 0.0068N/m^3$

Figure 8: LP curves using parameters associated with the two 2-extremum points and the birth point at $f_0 = 0.5N$. LP (dark blue solid line), 1-extremum (black ■) corresponding to the birth and the merging of ISs, 2-extremum (red ▲) corresponding to coincident birth and merging of ISs.

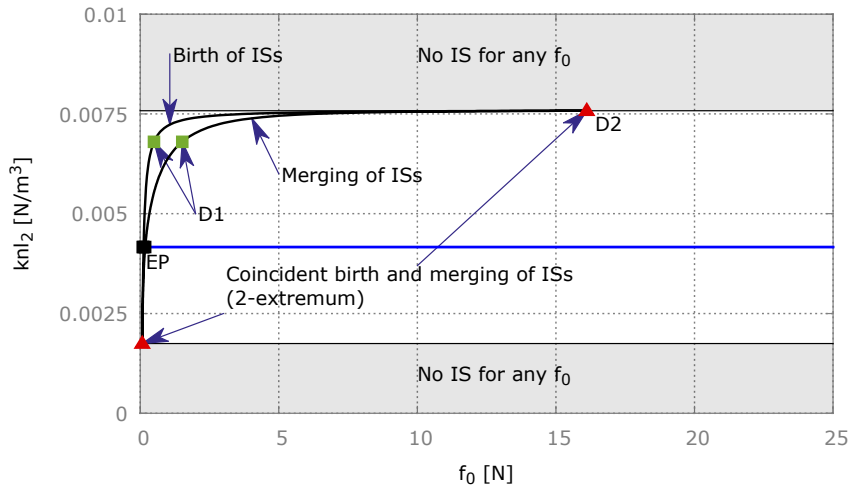
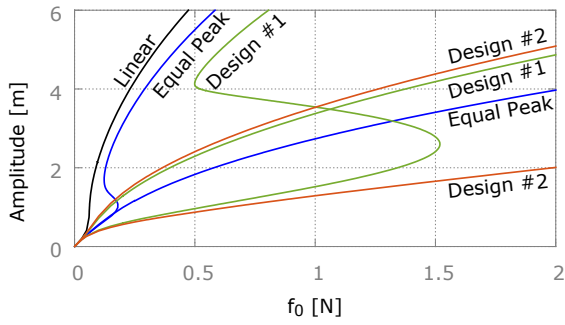
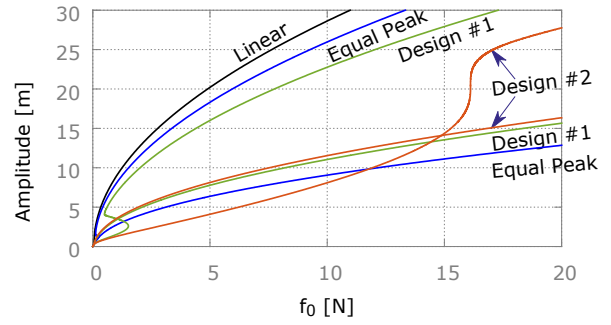


Figure 9: Projection of the branch of birth and merging points (1-extremum) on the knl_2 - f_0 plane. LP (dark blue) for $knl_2 \approx 0.0042N/m^3$, 1-extremum (black ■), 2-extremum (red ▲)



(a) Comparison of the maximum of amplitude.



(b) Comparison of the maximum of amplitude (extended view).

Figure 10: Continuation of the maximum of amplitude. Linear for $knl_2 = 0N/m^3$ (black), Equal Peak for $knl_2 = 0.0042N/m^3$ (blue), Birth of $f_0 = 0.5N$ for $knl_2 \approx 0.0068N/m^3$ (green), 2-extremum for $knl_2 \approx 0.0076N/m^3$ (orange)

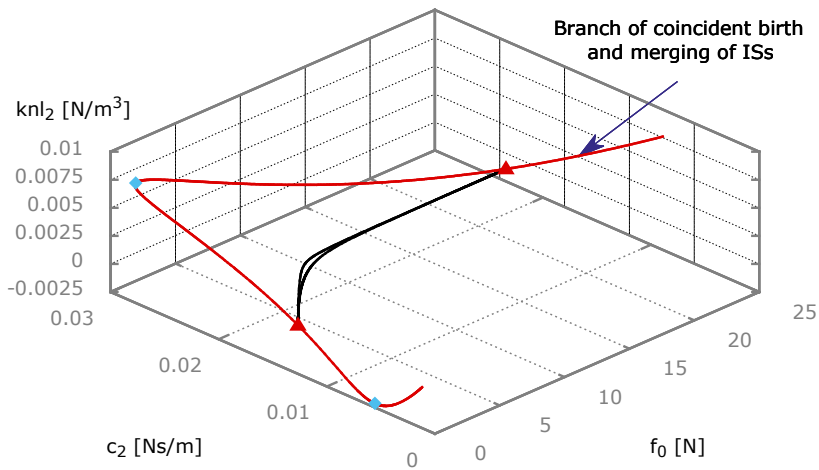
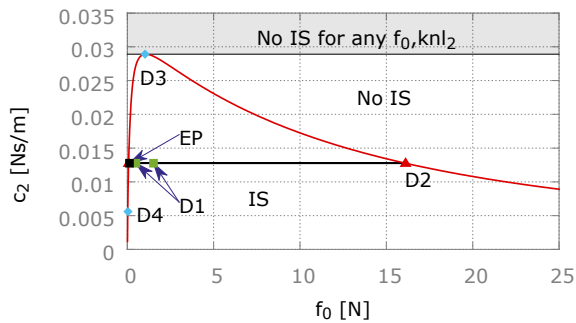
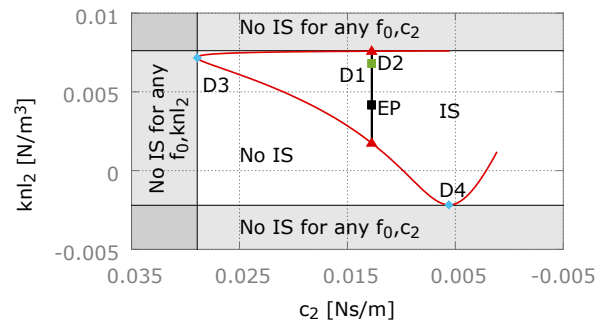


Figure 11: Continuation of 2-extremum points. 1-extremum (black), 2-extremum (red ▲), 3-extremum (light blue ◆)



(a) Projection on the c_2 - f_0 plane



(b) Projection on the knl_2 - c_2 plane

Figure 12: Projections of the branch of 2-extremum points. 1-extremum (black ■), 2-extremum (red ▲), 3-extremum (light blue ◆)

It is clear from these figures that the "safe" region is shrunked in the first case (Fig. 8a) whereas it is considerably enlarged in the second case (Fig. 8b). In addition, after projecting the 1-extremum branch of Fig. 7b onto the knl_2 - f_0 plane, see Fig. 9, there is no IS in the frequency response curves for $knl_2 > 0.0076N/m^3$ or $knl_2 < 0.0017N/m^3$ whatever the value of the other level-2 varying parameter f_0 . Moreover, this projected 1-extremum branch can be used to identify the value of knl_2 required to set the birth of ISs at specific amplitude of forcing f_0 between the upper and lower limit of existence of ISs. For instance, the IS birth can be set at $f_0 = 0.5N$ by choosing $knl_2 \approx 0.0068N/m^3$, as shown in Fig. 8c. This confirms the possibility of tuning the birth or merging point of ISs at a specific amplitude of forcing f_0 .

The efficiency of the vibration absorber of Fig. 8c can be verified by comparing the maximum of amplitude of the different designs. It can be observed in Fig. 10 that the equal peak design is the more efficient design before reaching its IS merging point. However, once the merging point of the equal peak design is crossed, the design with the set of parameters obtained for a birth point at $f_0 = 0.5N$ (Design #1) becomes more efficient. In the same way, once the merging point of the the design with the set of parameters obtained for a birth point at $f_0 = 0.5N$ is crossed, the design obtained at the 2-extremum at high amplitude of forcing (Design #2) becomes more efficient. As a results, the design of the NLTVA can be optimized by appropriately choosing the value of knl_2 according to the operating range of the forcing f_0 .

3.4. Level-3 of continuation: continuation of the coincident birth and merging points of ISs

At level-3 of the recursive continuation, the two 2-extremum points are tracked by considering the NLTVA damping coefficient c_2 as a new unknown in the extended system $\mathbf{G}_2(\mathbf{Y}_2, \alpha_2) = 0$. The subset of varying parameters at level-3 is then (f_0, knl_2, c_2) . The resulting branch of 2-extremum points is plotted in Fig. 11. All the points of this branch provide a set of parameters (f_0, knl_2, c_2) for which the birth and merging of ISs are coincident (no "unsafe" region). The projections of this branch on the c_2 - f_0 and c_2 - knl_2 planes are displayed in Figs. 12a and 12b. Using the extended system (11) at level-3 $\mathbf{G}_3(\mathbf{Y}_3) = \mathbf{0}$, several 3-extremum points are detected on this branch. Two 3-extremum points with respect to c_2 and knl_2 are obtained for $(c_2 = 0.029Ns/m, knl_2 = 0.072N/m^3, f_0 = 1.03N)$ and $(c_2 = 0.0056Ns/m, knl_2 = -0.0022N/m^3, f_0 = 0.036N)$ respectively. The 3-extremum point with respect to c_2 (Design #3) represents the upper limit of existence of ISs with respect to c_2 . Therefore, for $c_2 > 0.029Ns/m$, there is no IS whatever the value of the other level-3 varying parameters (f_0, knl_2) . In the same way, the 3-extremum point with respect to knl_2 (Design #4) represents the lower limit of existence of IS with respect to knl_2 . Consequently, for $knl_2 < -0.0022N/m^3$, there is no IS whatever the value of the other level-3 varying parameters (f_0, c_2) . However, the safe region is very small on this case ($f_0 = 0N$ to $0.026N$) and the practical realization of such a negative stiffness is not a trivial task. Therefore, this design is not very attractive. For high values of f_0 , the damping c_2 and nonlinear stiffness knl_2 coefficients tend to $c_2 = 0Ns/m$ and $knl_2 \approx 0.0076N/m^3$. The corresponding set of parameters is not usable since a system with zero damping is not efficient anymore and may not lead to a periodic solution over time. Above this asymptotic value of knl_2 , there is no IS whatever the value of (f_0, c_2) . It is noteworthy that the highest 2-extremum point of Fig. 12 is close to this asymptotic value of knl_2 . Therefore, the presence of ISs at this point is almost not influenced by the variation of c_2 .

3.5. Suitability of the designs of interest

From the previous results, it appears that designs #1, #2 and #3 are potential good candidates for the optimization of the safe operating region of the NLTVA. The corresponding sets of parameters (f_0, knl_2, c_2) are indicated with labels D1, D2 and D3 in Fig. 12 and gathered in Tab. 2 in order to make their comparison easier. Here, the value of f_0 corresponds to the end of the safe region, i.e., either the birth of ISs (Design #1) or the coincident birth and merging of ISs (Designs #2 and #3). It can also be read as a measure of the width of the safe region. It can be observed that the values of (knl_2, c_2) obtained with equal peak and other designs have the same order of magnitude, but these designs lead to significantly different values of f_0 at IS birth, i.e., to safe regions of very different width.

The maximum of amplitude of the primary mass for these three designs is plotted in Fig. 13 together with the results of the linear vibration absorber ($knl_2 = 0$) and the NLTVA with equal peak design. It is used to assess the efficiency of the absorber with the tested designs.

Form this figure, it can be concluded that the equal peak design is the most efficient one in the range $f_0 = [0N - 0.12N]$, i.e., in its safe region as defined in Fig. 4. Above $f_0 = 0.12N$, the other designs are much more efficient.

	Equal Peak (EP)	Design #1 (D1)	Design #2 (D2)	Design #3 (D3)
$c_2[Ns/m]$	0.0128	0.0128 (idem)	0.0128 (idem)	0.029 (+127%)
$kn_2[N/m^3]$	0.042	0.0068 (+62%)	0.0076 (+81%)	0.0072 (+71%)
$f_0[N]$ at IS birth	0.12	0.5 ($\times 4$)	16 ($\times 130$)	1.03 ($\times 9$)

Table 2: Comparison of the designs of interest. The equal peak (EP) design is used as reference. Relative differences with the EP design are indicated in parentheses

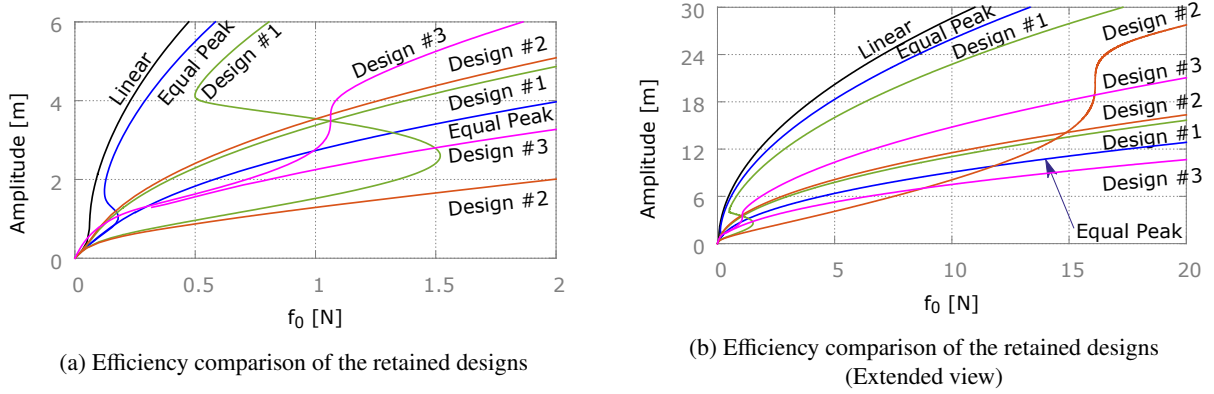


Figure 13: Continuation of the maximum of amplitude. Linear for $kn_2 = 0N/m^3$ (black), Equal Peak for $kn_2 = 0.0042N/m^3$ (blue), Birth of $f_0 = 0.5N$ for $kn_2 \approx 0.0068N/m^3$ (green), 2-extremum for $kn_2 \approx 0.0076N/m^3$ (orange), 3-extremum for $(kn_2, c_2) \approx (0.0072N/m^3, 0.029Ns/m)$ (Purple)

Design #2 seems superior to design #1 because it gives almost the same amplitude but has a much wider safe region (up to $f_0 = 16N$ instead of $0.5N$) while decorrelating the birth of IS from the damping coefficient c_2 . Finally, design #3 might be considered as the best compromise since it provides the lowest amplitude in its safe region up to $f_0 = 1.03N$ while decorrelating the birth of IS from the nonlinear stiffness coefficient kn_2 . In comparison with the equal peak design, its safe region is 9 times wider. However, this design has the worse performance in the range $f_0 = [0N - 0.1N]$. A way of improvement may consist in using hybrid active/passive control to switch from one design to another one depending on the value of the forcing amplitude f_0 .

To sum up, the multi-parametric recursive continuation method provides useful information by exploring the topology of the NLTVA ISs such as extremum points and regions of existence. The tested designs have a larger safe region leading to a larger operating range. Moreover, their vibration absorption efficiency is better than the equal peak design for high values of forcing. Designs #2 and #3 provide robustness by limiting the influence of c_2 and kn_2 respectively. Design #3 is particularly interesting because the appearance of ISs is decorrelated from the nonlinear stiffness coefficient kn_2 while keeping a better efficiency than other designs for high amplitudes of forcing. A perspective for improving the NLTVA would be to track LPs with respect to the mass ratio ϵ under equal peak constraint.

4. Conclusion

In this paper, an original and efficient multi-parametric recursive continuation algorithm is proposed. The method is based on a sequentially extending system characterizing extremum points in increasing codimensions. By applying this recursive continuation to a specific point of a system, its topology and all its extremums with respect to the chosen parameters are obtained. The information obtained with this topological exploration can then be used to optimize the system. Applied to a nonlinear vibration absorber, it is shown that this algorithm provides the limits of existence of isolated solutions with respect to a predefined set of system parameters. Using this information, the robustness of the absorber can be improved by enlarging the safe operating region without isolated solutions, while preserving the efficiency of the absorber and by decorrelating the appearance of isolated solutions from some system parameters.

Acknowledgements

This research was funded by a PhD Research Fellowship from the French Ministry of Higher Education and Research (MESR).

Conflicts of Interest

The authors declare that there are no conflicts of interest regarding the publication of this paper.

References

- [1] P. Sundararajan and S.T. Noah. Dynamics of forced nonlinear systems using shooting/arc-length continuation method - application to rotor systems. *Journal of vibration and acoustics*, 119(1):9–20, 1997.
- [2] A. H. Nayfeh and B. Balachandran. *Applied Nonlinear Dynamics: Analytical, Computational and Experimental Methods*. John Wiley & Sons, 2008.
- [3] R. Seydel. *Practical Bifurcation and Stability Analysis*, volume 5 of *Interdisciplinary Applied Mathematics*. Springer, New York, NY, 3rd edition, 2010.
- [4] C. De Boor and B. Swartz. Collocation at gaussian points. *SIAM Journal on Numerical Analysis*, 10(4):582–606, 1973.
- [5] E.J. Doedel, A.R. Champneys, T.F. Fairgrieve, Y.A. Kuznetsov, Bj orn Sandstede, and X. Wang. *AUTO 97: Continuation and bifurcation software*, 1998.
- [6] E.J. Doedel, A.R. Champneys, F. Dercole, T.F. Fairgrieve, Y.A. Kuznetsov, B. Oldeman, R.C. Paffenroth, B. Sandstede, X.J. Wang, C.H. Zhang, et al. *AUTO-07P: Continuation and bifurcation software for ordinary differential equations*, 2007.
- [7] A. Dhooge, W. Govaerts, and Y. Kuznetsov. MATCONT: a MATLAB package for numerical bifurcation analysis of ODEs. *ACM Transactions on Mathematical Software (TOMS)*, 29(2):141–164, 2003.
- [8] U. Ascher, J. Christiansen, and R.D. Russell. A collocation solver for mixed order systems of boundary value problems. *Mathematics of Computation*, 33(146):659–679, 1979.
- [9] K. Engelborghs, T. Luzyanina, and G. Samaey. DDE-BIFTOOL: a Matlab package for bifurcation analysis of delay differential equations. *TW Report*, 305, 2000.
- [10] H. Dankowicz and F. Schilder. An extended continuation problem for bifurcation analysis in the presence of constraints. *Journal of Computational and Nonlinear Dynamics*, 6(3):031003, 2011.
- [11] T.M. Cameron and J.H. Griffin. An alternating frequency/time domain method for calculating the steady-state response of nonlinear dynamic systems. *Journal of applied mechanics*, 56(1):149–154, 1989.
- [12] M. Krack, L. Panning-von Scheidt, and J. Wallaschek. A high-order harmonic balance method for systems with distinct states. *Journal of Sound and Vibration*, 332(21):5476 – 5488, 2013.
- [13] S. Nacivet, C. Pierre, F. Thouverez, and L. Jezequel. A dynamic lagrangian frequency-time method for the vibration of dry-friction-damped systems. *Journal of Sound and Vibration*, 265(1):201 – 219, 2003.
- [14] F. Schreyer and R.I. Leine. A mixed shooting–harmonic balance method for unilaterally constrained mechanical systems. *Archive of Mechanical Engineering*, 63(2):297–314, 2016.
- [15] V. Jaumouillé, J.-J. Sinou, and B. Petitjean. An adaptive harmonic balance method for predicting the nonlinear dynamic responses of mechanical systems - application to bolted structures. *Journal of sound and vibration*, 329(19):4048–4067, 2010.
- [16] A. Grolet and F. Thouverez. On a new harmonic selection technique for harmonic balance method. *Mechanical Systems and Signal Processing*, 30:43 – 60, 2012.
- [17] F. Schilder, W. Vogt, S. Schreiber, and H.M. Osinga. Fourier methods for quasi-periodic oscillations. *International journal for numerical methods in engineering*, 67(5):629–671, 2006.
- [18] M. Guskov, J.-J. Sinou, and F. Thouverez. Multi-dimensional harmonic balance applied to rotor dynamics. *Mechanics Research Communications*, 35(8):537–545, 2008.
- [19] L. Peletan, S. Bague, M. Torkhani, and G. Jacquet-Richardet. Quasi-periodic harmonic balance method for rubbing self-induced vibrations in rotor–stator dynamics. *Nonlinear Dynamics*, 78(4):2501–2515, 2014.
- [20] B. Zhou, F. Thouverez, and D. Lenoir. A variable-coefficient harmonic balance method for the prediction of quasi-periodic response in nonlinear systems. *Mechanical Systems and Signal Processing*, 64–65:233 – 244, 2015.
- [21] M.A. Crisfield. A fast incremental/iterative solution procedure that handles snap-through. *Computers & Structures*, 13(1):55 – 62, 1981.
- [22] G. Von Groll and D.J. Ewins. The harmonic balance method with arc-length continuation in rotor/stator contact problems. *Journal of sound and vibration*, 241(2):223–233, 2001.
- [23] B. Cochelin and C. Vergez. A high order purely frequency-based harmonic balance formulation for continuation of periodic solutions. *Journal of Sound and Vibration*, 324(1-2):243 – 262, 2009.
- [24] R. Seydel. Numerical computation of branch points in ordinary differential equations. *Numerische Mathematik*, 32(1):51–68, 1979.
- [25] R. Seydel. Numerical computation of branch points in nonlinear equations. *Numerische Mathematik*, 33(3):339–352, 1979.
- [26] G. Moore and A. Spence. The calculation of turning points of nonlinear equations. *SIAM Journal on Numerical Analysis*, 17(4):567–576, 1980.
- [27] P. Wriggers and J.C. Simo. A general procedure for the direct computation of turning and bifurcation points. *International journal for numerical methods in engineering*, 30(1):155–176, 1990.
- [28] A. Griewank and G.W. Reddien. Characterization and computation of generalized turning points. *SIAM journal on numerical analysis*, 21(1):176–185, 1984.

- [29] W. Govaerts. Numerical bifurcation analysis for ODEs. *Journal of computational and applied mathematics*, 125(1-2):57–68, 2000.
- [30] J-M. Battini, C. Pacoste, and A. Eriksson. Improved minimal augmentation procedure for the direct computation of critical points. *Computer methods in applied mechanics and engineering*, 192(16-18):2169–2185, 2003.
- [31] E.P. Petrov. Analysis of bifurcations in multiharmonic analysis of nonlinear forced vibrations of gas turbine engine structures with friction and gaps. *Journal of Engineering for Gas Turbines and Power*, 138(10):102502, 2016.
- [32] L. Xie, S. Baguet, B. Prabel, and R. Dufour. Numerical tracking of limit points for direct parametric analysis in nonlinear rotordynamics. *Journal of Vibration and Acoustics*, 138(2):021007, 2016.
- [33] A. Jepson and A. Spence. Folds in solutions of two parameter systems and their calculation. Part I. *SIAM journal on numerical analysis*, 22(2):347–368, 1985.
- [34] A. Eriksson, C. Pacoste, and A. Zdunek. Numerical analysis of complex instability behaviour using incremental-iterative strategies. *Computer Methods in Applied Mechanics and Engineering*, 179(3-4):265–305, 1999.
- [35] S. Baguet and B. Cochelin. Stability of thin-shell structures and imperfection sensitivity analysis with the asymptotic numerical method. *Revue Européenne des Eléments Finis*, 11(2-4):493–509, 2002.
- [36] M. Rezaiee-Pajand and B. Moghaddasie. Stability boundaries of two-parameter non-linear elastic structures. *International Journal of Solids and Structures*, 51(5):1089–1102, 2014.
- [37] Y.A. Kuznetsov. *Elements of applied bifurcation theory*, volume 112. Springer Science & Business Media, 2013.
- [38] W. Govaerts. *Numerical methods for bifurcations of dynamical equilibria*, volume 66. Siam, 2000.
- [39] A.G. Salinger, E.A. Burroughs, R.P. Pawlowski, E.T. Phipps, and L.A. Romero. Bifurcation tracking algorithms and software for large scale applications. *International Journal of Bifurcation and Chaos*, 15(03):1015–1032, 2005.
- [40] T. Detroux, L. Renson, L. Masset, and G. Kerschen. The harmonic balance method for bifurcation analysis of large-scale nonlinear mechanical systems. *Computer Methods in Applied Mechanics and Engineering*, 296:18–38, 2015.
- [41] L. Xie, S. Baguet, B. Prabel, and R. Dufour. Bifurcation tracking by harmonic balance method for performance tuning of nonlinear dynamical systems. *Mechanical Systems and Signal Processing*, 88:445–461, 2016.
- [42] K.-M. Nguyen. *A continuation approach for solving nonlinear optimization problems with discrete variables*. Theses, Stanford university, 2002.
- [43] G. Destino and G.T.F. Abreu. Solving the source localization problem via global distance continuation. In *2009 IEEE International Conference on Communications Workshops*, pages 1–6. IEEE, 2009.
- [44] H. Mobahi and J.W. Fisher III. A theoretical analysis of optimization by gaussian continuation. In *Proceedings of the Twenty-Ninth AAAI Conference on Artificial Intelligence*, AAAI’15, pages 1205–1211. AAAI Press, 2015.
- [45] J.M. Hansen. Synthesis of spatial mechanisms using optimization and continuation methods. In *Computational Dynamics in Multibody Systems*, pages 183–196. Springer, 1995.
- [46] A.-X. Liu and T.-L. Yang. Finding all solutions to unconstrained nonlinear optimization for approximate synthesis of planar linkages using continuation method. *Journal of Mechanical Design*, 121(3):368–374, 1999.
- [47] J.R. Rao and P.Y. Papalambros. A non-linear programming continuation strategy for one parameter design optimization problems. In *Proceedings of ASME Design Automation Conference, Montreal, Quebec, Canada*, pages 77–89, 1989.
- [48] H.T. Jongen, P. Jonker, and F. Twilt. Critical sets in parametric optimization. *Mathematical programming*, 34(3):333–353, 1986.
- [49] J. Guddat, H. T. Jongen, and D. Nowack. Parametric optimization: pathfollowing with jumps. In *Approximation and Optimization*, pages 43–53. Springer, 1988.
- [50] D.M. Wolf and S.R. Sanders. Multiparameter homotopy methods for finding dc operating points of nonlinear circuits. *IEEE Transactions on Circuits and Systems I: Fundamental Theory and Applications*, 43(10):824–838, 1996.
- [51] F. Vanderbeck. A nested decomposition approach to a three-stage, two-dimensional cutting-stock problem. *Management Science*, 47(6):864–879, 2001.
- [52] O. Schütze, A. Dell’Aere, and M. Dellnitz. On continuation methods for the numerical treatment of multi-objective optimization problems. In *Dagstuhl Seminar Proceedings*. Schloss Dagstuhl-Leibniz-Zentrum für Informatik, 2005.
- [53] J.P. Kernevez, Y. Liu, M.L. Seoane, and E.J. Doedel. Optimization by continuation. In *Continuation and Bifurcations: Numerical Techniques and Applications*, pages 349–362. Springer, 1990.
- [54] B. Balaram, M.D. Narayanan, and P.K. Rajendrakumar. Optimal design of multi-parametric nonlinear systems using a parametric continuation based genetic algorithm approach. *Nonlinear Dynamics*, 67(4):2759–2777, 2012.
- [55] M. Wang. Feasibility study of nonlinear tuned mass damper for machining chatter suppression. *Journal of Sound and Vibration*, 330(9):1917–1930, 2011.
- [56] N. Carpineto, W. Lacarbonara, and F. Vestroni. Hysteretic tuned mass dampers for structural vibration mitigation. *Journal of Sound and Vibration*, 333(5):1302–1318, 2014.
- [57] G. Habib, T. Detroux, R. Vigué, and G. Kerschen. Nonlinear generalization of Den Hartog’s equal-peak method. *Mechanical Systems and Signal Processing*, 52-53:17 – 28, 2015.
- [58] A. Malher, C. Touzé, O. Doaré, G. Habib, and G. Kerschen. Flutter control of a two-degrees-of-freedom airfoil using a nonlinear tuned vibration absorber. *Journal of Computational and Nonlinear Dynamics*, 12(5):051016–051016–11, 2017.
- [59] H.N. Abramson. Response curves for a system with softening restoring force. *Journal of applied mechanics*, 22(3):434–435, 1955.
- [60] L.A. DiBerardino and H. Dankowicz. Accounting for nonlinearities in open-loop protocols for symmetry fault compensation. *Journal of Computational and Nonlinear Dynamics*, 9(2):021002, 2014.
- [61] F. Mangussi and D.H. Zanette. Internal resonance in a vibrating beam: a zoo of nonlinear resonance peaks. *PLoS one*, 11(9):e0162365, 2016.
- [62] S. Arroyo and D.H. Zanette. Duffing revisited: phase-shift control and internal resonance in self-sustained oscillators. *The European Physical Journal B*, 89(1):1–8, 2016.
- [63] G. Gatti, I. Kovacic, and M.J. Brennan. On the response of a harmonically excited two degree-of-freedom system consisting of a linear and a nonlinear quasi-zero stiffness oscillator. *Journal of Sound and Vibration*, 329(10):1823–1835, 2010.
- [64] G. Gatti. Uncovering inner detached resonance curves in coupled oscillators with nonlinearity. *Journal of Sound and Vibration*, 372:239–254,

2016.

- [65] G. Gatti. On the undamped vibration absorber with cubic stiffness characteristics. In *Journal of Physics: Conference Series*, volume 744, page 012225. IOP Publishing, 2016.
- [66] G. Gatti. Fundamental insight on the performance of a nonlinear tuned mass damper. *Meccanica*, 53(1-2):111–123, 2018.
- [67] T. Detroux, G. Habib, L. Masset, and G. Kerschen. Performance, robustness and sensitivity analysis of the nonlinear tuned vibration absorber. *Mechanical Systems and Signal Processing*, 60-61:799 – 809, 2015.
- [68] T.L. Hill, S.A. Neild, and A. Cammarano. An analytical approach for detecting isolated periodic solution branches in weakly nonlinear structures. *Journal of Sound and Vibration*, 379:150–165, 2016.
- [69] G. Habib, G.I. Cirillo, and G. Kerschen. Isolated resonances and nonlinear damping. *Nonlinear Dynamics*, pages 1–16, 2018.
- [70] G.I. Cirillo, G. Habib, G. Kerschen, and R. Sepulchre. Analysis and design of nonlinear resonances via singularity theory. *Journal of Sound and Vibration*, 392:295–306, 2017.
- [71] Y. Starosvetsky and O.V. Gendelman. Vibration absorption in systems with a nonlinear energy sink: nonlinear damping. *Journal of Sound and Vibration*, 324(3):916–939, 2009.
- [72] E. Gourc, G. Michon, S. Seguy, and A. Berlioz. Experimental investigation and design optimization of targeted energy transfer under periodic forcing. *Journal of Vibration and Acoustics*, 136(2):021021, 2014.